Molecular Cell, Vol. 8, 33–44, July, 2001, Copyright ©2001 by Cell Press

Precursor RNAs Harboring Nonsense Codons Accumulate Near the Site of Transcription

Oliver Mühlemann,[1,5,6] Caroline S. Mock-Casagrande,[1,5] Jun Wang,[2,5] Shulin Li,[2] Noélia Custódio,[3] Maria Carmo-Fonseca,[3] Miles F. Wilkinson,[2] and Melissa J. Moore[1,4]

[1] Howard Hughes Medical Institute
W.M. Keck Center for Cellular Visualization
Department of Biochemistry
Brandeis University
Waltham, Massachusetts 02454

[2] Department of Immunology
M.D. Anderson Cancer Center
University of Texas
Houston, Texas 77030

[3] Institute of Histology and Embryology
Faculty of Medicine
University of Lisbon
1699 Lisbon codex
Portugal

Summary

Messenger RNAs containing premature termination codons (PTCs) are selectively eliminated by nonsense-mediated mRNA decay (NMD). Paradoxically, although cytoplasmic ribosomes are the only known species capable of PTC recognition, in mammals many PTC-containing mRNAs are apparently eliminated prior to release from the nucleus. To determine whether PTCs can influence events within the nucleus proper, we studied the immunoglobulin (Ig)-μ and T cell receptor (TCR)-β genes using fluorescent in situ hybridization (FISH). Alleles containing PTCs, but not those containing a missense mutation or a frameshift followed by frame-correcting mutations, exhibited elevated levels of pre-mRNA, which accumulated at or near the site of transcription. Our data indicate that mRNA reading frame can influence events at or near the site of gene transcription.

Introduction

Nonsense-mediated mRNA decay (NMD) is a quality-control system that selectively eliminates messenger RNAs (mRNAs) containing premature termination codons (PTCs) (Maquat, 1995). Although the detailed mechanism of NMD has yet to be elucidated, it is known to be a posttranscriptional process that requires open reading frame (ORF) recognition (reviewed in Frischmeyer and Dietz, 1999; Hentze and Kulozik, 1999). Consistent with ORF recognition being carried out by ribosomes, biochemical separation of the nuclear and cytoplasmic compartments in vertebrate cells has shown that some mRNAs are degraded by NMD in the cytoplasm (Lim et al., 1992; Whitfield et al., 1994; Moriarty et al., 1998).

Despite evidence that NMD involves the translation machinery and can occur in the cytoplasm, most PTC+ mRNAs in metazoans are apparently eliminated prior to their release from the nucleus (reviewed in Maquat, 1995; Li and Wilkinson, 1998; Hentze and Kulozik, 1999). Included in this class are mRNAs encoding Ig-κ light chain (Lozano et al., 1994; Aoufouchi et al., 1996), TCR-β (Carter et al., 1995, 1996; Li et al., 1997), dihydrofolate reductase (Urlaub et al., 1989), adenine phosphoribosyltransferase (Kessler and Chasin, 1996), triose phosphate isomerase (Cheng and Maquat, 1993; Belgrader et al., 1994), v-src (Simpson and Stoltzfus, 1994), mouse major urinary protein (Belgrader and Maquat, 1994), β-globin (Baserga and Benz, 1992), and *Drosophila melanogaster* alcohol dehydrogenase (Brogna, 1999). For most of these transcripts, the presence of a PTC decreases the steady-state level of nuclear mRNA, but does not significantly alter the half-life of cytoplasmic mRNA (Belgrader et al., 1994; Carter et al., 1996).

Models put forward to explain how NMD could influence mRNA levels in the nuclear fraction of cells include (1) cotranslational export and (2) nuclear scanning (reviewed in Maquat, 1995; Li and Wilkinson, 1998; Hentze and Kulozik, 1999). The cotranslational export model posits that PTC recognition by the cytoplasmic translation machinery can trigger NMD before a PTC+ mRNA has completely transitted the nuclear pore. Thus, lower PTC+ mRNA levels are detected in the nuclear fraction even though NMD occurs in the cytoplasm. In contrast, the nuclear-scanning model posits that PTC recognition occurs within the nucleus proper, prior to mRNA export. Although this model is supported by several findings (Li and Wilkinson, 1998), it necessitates the existence of a nuclear frame reader, possibly nuclear ribosomes, which is contrary to the prevailing belief that *only* the cytoplasmic translation machinery is capable of detecting and responding to ORFs.

Also linking NMD to nuclear events are documented associations between NMD and pre-mRNA splicing. In vertebrate cells, PTCs are distinguished from normal stop codons by their position relative to the last intron. That is, if a termination codon is located upstream of at least one exon-exon junction, it is identified as a PTC and the mRNA is targeted for decay (Carter et al., 1996; Thermann et al., 1998; Zhang et al., 1998a,b; reviewed in Li and Wilkinson, 1998; Nagy and Maquat, 1998; Hentze and Kulozik, 1999). The mechanism by which this occurs likely involves splicing-dependent alterations in the proteins associated with mRNAs (Le Hir et al., 2000 and references therein). Intriguingly, some studies have suggested that PTCs can affect the splicing process directly, either by inhibiting splicing or regulating splice site selection (Dietz et al., 1993; Dietz and Kendzior, 1994; Lozano et al., 1994; Aoufouchi et al., 1996; Gersappe et al., 1999). However, in many cases, these effects result from the chance disruption of an exonic splicing enhancer by the mutation that also generated the PTC (Cooper and Mattox, 1997; Shiga et al., 1997; Hentze and Kulozik, 1999; Liu et al., 2001).

Here, we report the use of fluorescent in situ hybridiza-

[4] Correspondence: mmoore@brandeis.edu
[5] These authors contributed equally to this work.
[6] Present address: Institute of Cell Biology, University of Bern, Baltzerstrasse 4, CH-3012 Bern, Switzerland.

tion (FISH) and ribonuclease protection (RPA) to examine the subcellular localization and processing state of PTC− (wild-type) and PTC+ RNAs. To avoid possible artifacts, we used only quantitative techniques that assay RNA directly without signal amplification. We worked with two experimental systems well-documented to undergo efficient NMD: mouse B cells expressing endogenous Ig-μ genes (Connor et al., 1993; 1994) and HeLa cells transfected with mouse TCR-β mini-gene constructs (Carter et al., 1996; Li et al., 1997). Prior to FISH and RPA analysis, both systems were carefully characterized in terms of their relative transcription rates and steady-state mRNA levels. Remarkably, in both systems we detected larger and brighter fluorescent foci in the nuclei of cells expressing a PTC+ allele than in cells expressing the corresponding PTC− allele. Consistent with these foci being the sites of transcription, they were deep within the nuclear interior. RPA revealed that these bright nuclear foci result from increased accumulation of unspliced RNA from PTC+ alleles. This pre-mRNA accumulation was observed with nonsense codons and frameshift-induced PTCs, but not with a missense codon or with frameshift combinations that restored ORF integrity. Our study therefore demonstrates that disruption of mRNA reading frame can have *intranuclear* consequences for RNA metabolism.

Results

Transcriptionally-Matched B-Cell Lines Expressing Wild-Type and Mutant Alleles of the Endogenous Ig-μ Gene

A set of B-cell lines derived from the well-studied mouse Sp6/HL hybridoma was chosen for initial FISH analysis. The set consisted of the parental PTC− (Sp6) hybridoma, which contains a single functionally rearranged μ gene, derivative cell lines (N89, N114, U30, and X54) harboring PTCs in three different exons, and a control line in which the entire μ gene had been deleted (X10) (Figure 1A) (Connor et al., 1993; 1994).

Prior to FISH analysis, we measured the relative μ transcription rates and steady-state μ mRNA levels in each cell line. Nuclear run-on experiments revealed that the μ transcription rate in every PTC+ cell line was experimentally indistinguishable from that of the PTC− Sp6 cell line (Figures 1B and 1C). Northern blot analysis of either total RNA (Figure 1D) or poly(A)$^+$ RNA (data not shown) showed that the PTC+ N114, U30, and X54 cell lines contained 18- to 60-fold less μ mRNA than the PTC− Sp6 cell line. Thus, these PTC+ μ transcripts are efficiently eliminated by NMD. In contrast, the PTC+ N89 cell line contained only 2-fold less μ mRNA than the Sp6 cell line, as observed previously (Buzina and Shulman, 1999). X10 cells exhibited no significant run-on or northern signals with μ probes, consistent with complete deletion of the μ locus in this line.

Ig-μ Transcripts Harboring PTCs Accumulate at or Near the Site of Transcription

We next examined intracellular μ RNA localization by FISH. To do so, equal numbers of exponentially growing PTC− Sp6 cells and cells from a single PTC+ line were mixed and allowed to adhere to coverslips. Following fixation, cells were hybridized under nondenaturing conditions using directly-labeled, rhodamine-containing FISH probes (red). Subsequent incubation with FITC-coupled, anti-IgM antibody (green) allowed distinction between the PTC− IgM+ Sp6 cells and PTC+ IgM− cells. Having PTC− and PTC+ cells on the same coverslip enabled us to compare FISH signals in side-by-side cells. Thus, possible artifacts from variable hybridization efficiencies between coverslips or even different areas on the same coverslip were effectively eliminated. Because the rhodamine FISH signal was mostly nuclear, while the FITC anti-IgM antibody detected IgM on the cell surface, no interference between the green and red signals was observed (data not shown).

Because the local concentration of a given transcript is usually highest at its site of synthesis, FISH often reveals the transcription site as a bright spot within the nuclear interior (Lawrence et al., 1989; Dirks et al., 1995; Jolly et al., 1998; Custodio et al., 1999). When hybridized with a genomic μ probe, the majority of hybridoma cells expressing either a PTC− or PTC+ μ allele did exhibit a single spot of intense fluorescence (Figure 2A). DNA labeling with Hoechst dye (blue) and 3D analysis through multiple focal planes revealed that this locus was clearly internal to the nucleus, consistent with it being the site of μ gene transcription. No FISH signal was observed in Ig-μ$^-$ X10 cells.

Surprisingly, the nuclear FISH spots were larger and brighter on average in the four PTC+ cell lines than in the PTC− Sp6 line. To quantify these differences, deconvolved 3D images were projected onto a single plane. With only the red (FISH) channel active, each cell was judged by eye to contain a bright nuclear spot, a dim spot, or no spot at all. Subsequently, PTC− and PTC+ cells were identified by overlaying the green (anti-IgM FITC) signal. This method allowed for the rapid analysis of many cells (between 40 and 198 from randomly selected fields) while avoiding any bias in the assessment of spot intensities. Whereas 25% to 40% of PTC+ cells had "bright spots," fewer than 10% of the PTC− Sp6 cells were in this category (Figure 2B). Conversely, whereas 10% or fewer of the PTC+ cells contained no detectable nuclear spot, approximately 25% of Sp6 cells lacked a spot. Thus, B cells expressing PTC+ μ alleles appear to accumulate higher levels of μ RNA at or near the site of transcription than do B cells expressing a PTC− μ allele. Furthermore, the degree of intranuclear RNA accumulation is independent of PTC position within the μ gene.

Three of the four cell lines containing a PTC+ μ allele were generated by random mutagenesis using either X-rays (X54) or nitrosoguanidine (N89, N114) (Connor et al., 1993). Thus, it was theoretically possible that nuclear μ RNA accumulation in these mutagenized cell lines resulted from defects in other genes, such as genes required for RNA processing, rather than from the documented nonsense mutations in the μ gene. However, Northern blotting and FISH analyses for Ig J-chain RNA revealed no significant differences in J-chain mRNA levels or transcription spot intensities among any of the cell lines (data not shown).

Elevated Levels of Unspliced Transcripts from Ig-μ Genes Harboring PTCs

To assess whether the RNA accumulating at PTC+ μ loci contained introns, we performed FISH with a probe

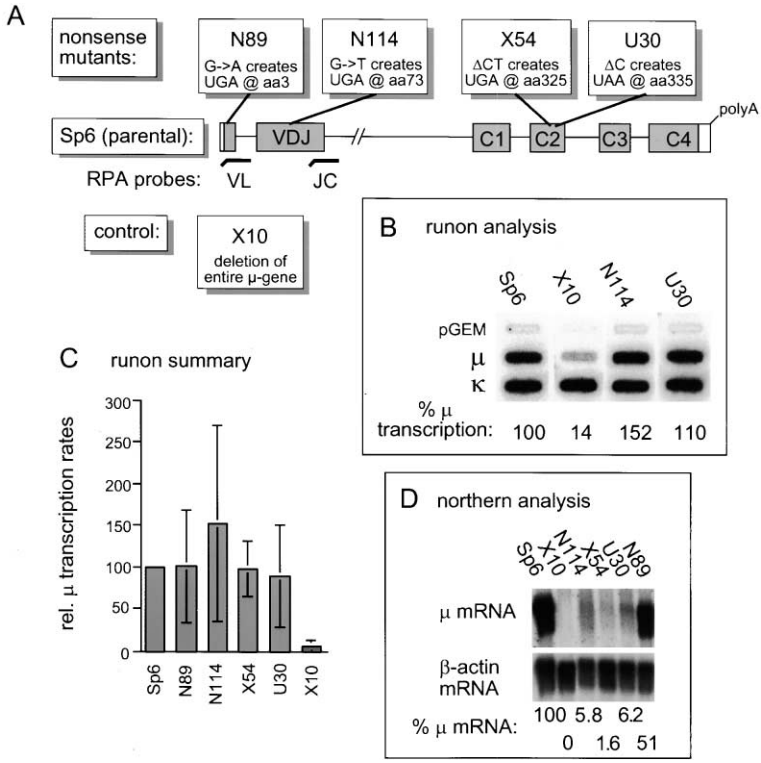

Figure 1. Parental and Mutant Ig-μ Genes and RNA Characterization by Nuclear Run-On and Northern Blot Analyses

(A) Schematic illustration of Ig-μ pre-mRNA for the secreted isoform. Boxes, and thin and thick lines depict exons, introns, and probes for RNase protection assays, respectively. The full-length ORF present in Sp6 is indicated by gray shading. For mutant cells lines, mutations and PTC positions are indicated.

(B) Typical nuclear run-on assay. Newly synthesized, [^{32}P]-labeled transcripts from indicated cell lines were hybridized to linearized, denatured plasmid DNA containing the μ gene (pRSp6), the κ gene (pRTk1), or the empty pGEM vector, which controlled for nonspecific background hybridization. In other experiments (not shown), mouse β-actin cDNA was included for normalization.

(C) Summary of nuclear run-on assays. Relative μ transcription rates were normalized to the sum of κ and β-actin signals. Average values of at least three experiments are shown for each cell line; error bars indicate standard deviations.

(D) Northern analysis of Ig-μ and β-actin mRNAs in total cellular RNA (5 μg). Relative μ mRNA levels were normalized to β-actin mRNA.

against the JC intron. As did the genomic probe, this intron-specific probe hybridized with a single locus of high intensity fluorescence in the nuclei of most cells containing the μ gene, while no specific fluorescence was detected in Ig-μ$^-$ X10 cells (Figure 2C). Remarkably, the difference in brightness of the nuclear signal in PTC− and PTC+ cells was even more pronounced with the intronic probe (Figure 2C) than with the genomic probe (Figure 2A). With the intronic probe, the bright nuclear spots in PTC+ cells were often surrounded by a cloud of smaller satellite spots. Quantitative analysis of these intronic FISH signals, performed as previously described, yielded very similar results (Figure 2D) to those observed with the genomic probe (Figure 2B).

To further substantiate the differences, we performed a more detailed quantitative comparison of three-dimensional volumes and total fluorescence intensities of nuclear spots in N114 and Sp6 cells. Consistent with the results from our more qualitative approach above, cumulative histograms revealed that spots in N114 cells generally occupied larger volumes and were more intense than those in Sp6 cells (Figure 3), with the total volumes and intensities being highly correlative for both cell types. The mean spot volume and mean spot intensity were both three times higher for N114 cells than Sp6 cells (data not shown). Thus, PTC+ μ RNA does accumulate within the nucleus and most of the accumulated RNA contains the JC intron.

The above observations suggested that the intranuclear RNA accumulating in PTC+ cell lines might be unspliced. To examine this, we employed ribonuclease protection analysis (RPA) with riboprobes complementary to the 5′ splice site region of the VL and JC introns (see Figure 1A and Experimental Procedures) to quantify both spliced and unspliced μ RNA (Figure 4A). Consistent with the Northern analysis (Figure 1D), RPA showed that spliced μ mRNA levels were 15- to 45-fold lower in the N114, X54, and U30 PTC+ cell lines than in the PTC− Sp6 cell line, whereas N89 PTC+ cells showed only a 1.5- to 1.8-fold decrease in μ mRNA. In contrast, unspliced μ RNA levels were elevated in all four PTC+ cell lines (by an average of 5-fold) compared with the PTC− Sp6 cell line (Figure 4). Paralleling the FISH results, the degree of this pre-mRNA elevation was independent of PTC position within the gene. Furthermore, in all four PTC+ cell lines, similar levels of unspliced RNA were detected with both the VL and JC intron probes. Taken together, these results suggest that the presence of a PTC leads to decreased pre-mRNA processing efficiency at the Ig-μ locus.

Elevated Levels of Unspliced Transcripts from a TCR-β Gene Harboring a PTC

To assess whether intranuclear accumulation of unspliced PTC+ RNA is a general phenomenon or is specific to Ig-μ transcripts in B cells, we next examined PTC− and PTC+ variants of a TCR-β gene whose transcripts are strongly downregulated in response to PTCs in both T cells and HeLa cells (Carter et al., 1995, 1996; Li et al., 1997). For this study, we generated stably transfected HeLa cell clones expressing PTC− and PTC+ versions of a TCR-β minigene under control of the human β-actin promoter (Figure 5A). We analyzed five randomly selected clones: 3C1 and 3C3 expressing the PTC− version, and 7C3, 7C5, and 7C6 expressing a PTC+ version that contains a nonsense mutation at codon 68.

Nuclear run-on assays (Figure 5B) revealed that all five cell clones exhibited very similar TCR-β transcription rates, ranging between 0.9 and 1.3 relative to the

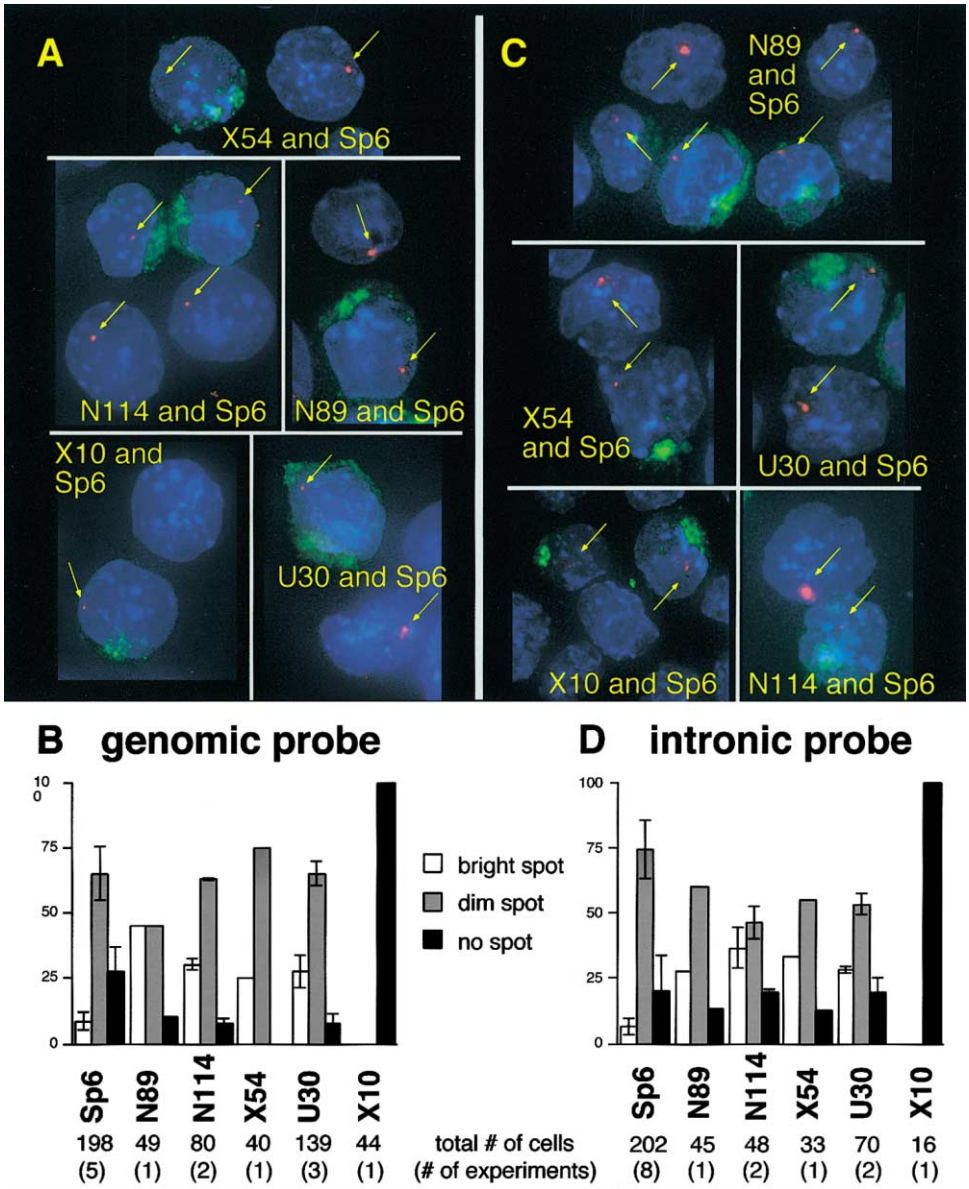

Figure 2. In Situ Visualization of μ RNA in Side-By-Side Parental (Sp6) and Mutant Cells with Genomic and Intronic μ Probes

(A) Parental (Sp6) and mutant Ig-μ cells hybridized with rhodamine-labeled genomic μ probe (red) and stained with FITC-coupled anti-IgM antibody (to selectively detect Sp6 cells, green) and Hoechst dye (to stain DNA, blue). Shown here are deconvolved images projected onto a single plane. Arrows indicate fluorescent signals at transcription sites.

(B) Summary of FISH quantifications with the genomic μ probe (see Results for details). Bars represent average percentages of the three classes (no, dim, or bright spot) for each cell line. When only two experiments contributed to the average, error bars represent the range; otherwise error bars reflect standard deviation.

(C) Same as in (A), except with a rhodamine-labeled probe against the JC intron.

(D) Summary of FISH quantifications with the JC intron probe.

PTC− 3C3 clone. However, Northern blotting showed that steady-state TCR-β mRNA levels were dramatically lower (25- to 50-fold) in the PTC+ cell clones than in the PTC− cell clones (Figure 5C). This magnitude of downregulation is similar to that previously reported for these same constructs when transiently transfected into HeLa cells (Li et al., 1997).

We next examined the subcellular distribution of TCR-β RNA by FISH (Figure 6). In all five stably transfected cell clones, the majority of cells exhibited a single spot of high intensity fluorescence in the nucleus (panels 1–2 and 4–6), indicating that the transfected genes had integrated at a single site in each clone. This was confirmed by performing hybridizations with a probe derived from the expression vector alone under conditions where only the transfected DNA could be detected (i.e., after RNase digestion and DNA denaturation; data not shown). The signals arising from TCR-β probes were specific to TCR-β transcripts, as very little signal was detected in untransfected HeLa cells (panel 3) and the

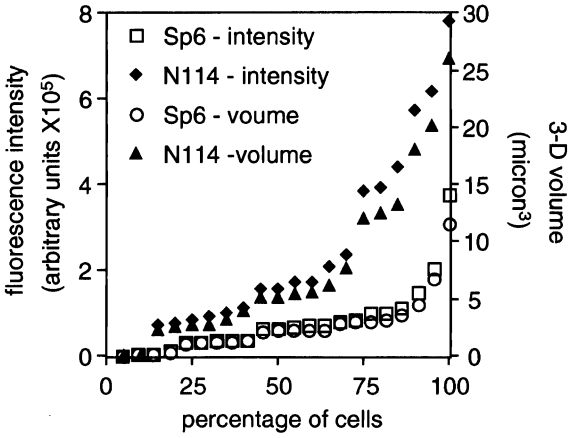

Figure 3. Quantification of Transcription Spots in Sp6 and N114 Cells

The three-dimensional volumes and total fluorescence intensities of transcription spots in N114 and Sp6 cells from one FISH experiment were measured as in Experimental Procedures. Cumulative histograms show the percentage of cells having spots equal to or less than a given volume (right axis) or total intensity (left axis).

FISH signals in minigene-containing cells were sensitive to RNase treatment (data not shown). Remarkably, paralleling the results with the B-cell lines, HeLa cells expressing the PTC+ TCR-β construct again had generally larger and brighter transcription spots than did the corresponding PTC− cells (Figure 6).

To test whether the brighter nuclear TCR-β FISH signals reflected increased pre-mRNA levels in the PTC+ cell clones, we performed RPA on total RNA from each clone. Consistent with Northern analysis (Figure 5C), RPA indicated that spliced TCR-β mRNA levels were 38- to 63-fold lower in the PTC+ clones than in the PTC− clones (Figure 7A). Conversely, the level of unspliced RNA was two to five times higher in the three PTC+ cell clones than in the two PTC− cell clones (Figure 7B). Both VL and JC intron probes yielded almost identical results (Figure 7B and data not shown). Thus, the presence of the PTC correlated with increased levels of pre-mRNA containing introns to either side of the PTC-bearing exon. Because these findings parallel those observed with B-cell lines expressing PTC− and PTC+ Ig-μ alleles, intranuclear accumulation of unspliced transcripts from PTC+ genes is apparently neither gene nor cell line specific.

Accumulation of Unspliced RNA from PTC+ Genes Depends on the Reading Frame

Our results suggest that Ig-μ and TCR-β transcripts harboring nonsense codons may be less efficiently processed than transcripts encoding mRNAs with full-length open reading frames. One well-documented mechanism by which nonsense mutations can affect pre-mRNA processing is by the disruption of exonic splicing enhancers (ESEs; Maquat, 1996; Valentine, 1998; Liu et al., 2001). If disruption of an ESE is responsible for a pre-mRNA splicing effect caused by a nonsense mutation, then a missense or silent mutation at the same site can have similar consequences (Liu et al., 2001).

To test this possibility, we generated stably transfected HeLa cell lines expressing a wild-type (A) TCR-β construct or one containing either a missense (B) or nonsense (C) mutation at codon 120. Relative mRNA and pre-mRNA levels were determined by RPA of total nuclear and cytoplasmic RNA (Figure 8A). Spliced mRNA was present in both the nuclear and cytoplasmic fractions. For the PTC+ cell line, lower levels of spliced mRNA were apparent in both compartments, consistent with our previous studies showing that PTC+ TCR-β

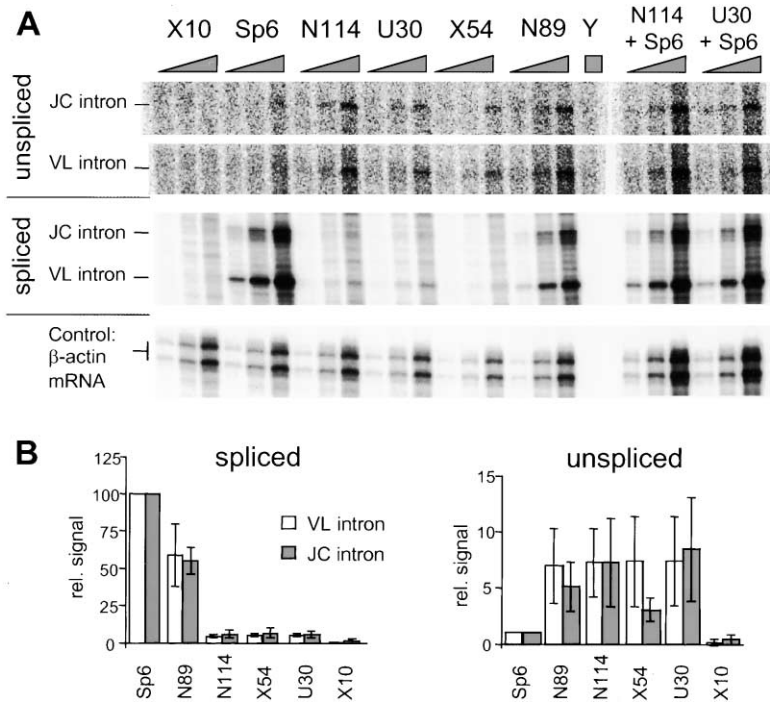

Figure 4. Quantification of Spliced and Unspliced PTC− and PTC+ Ig-μ RNA by RNase Protection Analysis

(A) Example of RPA data. Total RNA (0.66 μg, 2 μg, and 6 μg) from indicated B-cell lines was hybridized with [^{32}P]-labeled VL and JC (Figure 1A; 12 fmol, each) and mouse β-actin (see Experimental Procedures; 10 fmol) riboprobes. Yeast RNA (Y; 6 μg) served as negative control. In right-most lanes, equal amounts of Sp6 RNA and N114 or U30 RNA (0.66 μg, 2 μg, and 6 μg, each) were mixed to demonstrate that RPA probes were not limiting. All sections are from a single gel; the image contrast was enhanced in upper panels allow visualization of faint unspliced RNA signals. β-actin mRNA (double band) was used for normalization.

(B) Summary of RNase protection analyses. Average values relative to Sp6 from at least four experiments are shown for spliced (left) and unspliced (right) signals. Error bars represent standard deviations.

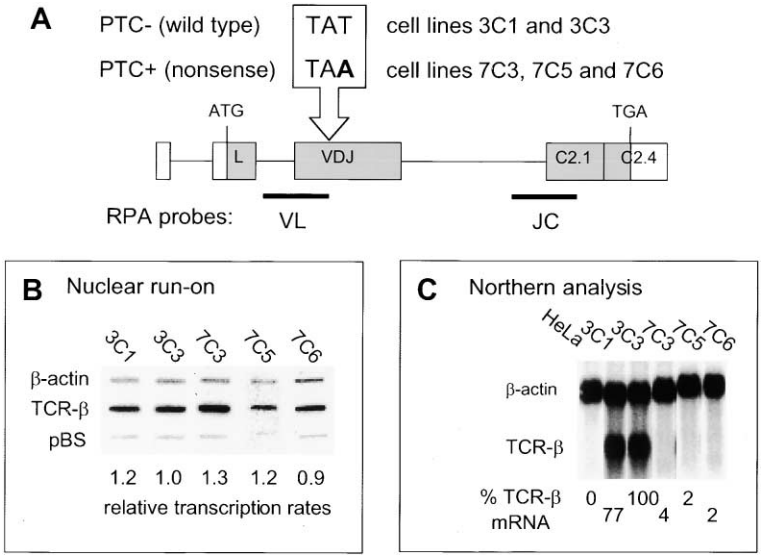

Figure 5. Characterization by Nuclear Run-On and Northern Blot Analyses of HeLa Cell Lines Stably Transfected with TCR-β Minigene Constructs

(A) Schematic illustration of PTC+ and PTC− TCR-β constructs used for Figures 5–7. Boxes and thin and thick lines depict exons, introns, and probes for RNase protection assays, respectively. The PTC− minigene ORF is indicated by gray shading. The PTC (TAA) is located at amino acid 68.

(B) Nuclear run-on assay. Newly synthesized [^{32}P]-labeled transcripts from PTC− (3C1 and 3C3) and PTC+ (7C3, 7C5, and 7C6) cell lines were hybridized to denatured, nicked plasmid DNAs specific to human β-actin exon 2, the TCR-β sequence of the minigene, and the empty pBS-SK+ vector. The pBS-SK+ vector controlled for nonspecific background hybridization and β-actin was used to normalize TCR-β signals. Numbers represent average relative transcription rates from two experiments.

(C) Northern blot analysis of 5 μg total RNA from indicated cell lines. The β-actin signal was used for normalization of TCR-β mRNA signals.

mRNAs are downregulated in the nuclear fraction (Carter et al., 1996). However, the PTC+ cell line clearly contained higher levels of nuclear pre-mRNA than did either the PTC− or missense cell line.

Although these results demonstrated that a missense mutation at TCR-β codon 120 did not replicate the pre-mRNA accumulation effect of a nonsense mutation at the same position, it remained possible that the G → A change generating the missense codon was less disruptive of an ESE than the G → T change generating the nonsense codon. To examine this possibility, we next tested the effects of insertion mutations. Introduction of a 10 nt insert into the VDJ exon generated a PTC in the following exon (codon 148; Figure 8B, construct D). As had all previous mutations that created PTCs, this construct expressed both a lower level of spliced TCR-β mRNA and an elevated level of unspliced TCR-β RNA relative to the PTC− construct (construct A; Figure 8). In contrast, introduction of a 9 nt (in-frame) insert at the same position (construct E) yielded spliced and unspliced RNA levels that were indistinguishable from construct A. Because both 9 nt and 10 nt insertions would be expected to disrupt any ESE at the insertion site equally, this result suggested that pre-mRNA accumulation was a consequence of reading frame alteration rather than ESE disruption. If so, it should be possible to suppress the effect of the 10 nt insertion by restoring the reading frame to the normal ORF prior to codon 148 (the PTC position in construct D). To test this, we deleted one nucleotide in either the VDJ or Cβ2.1 exon of construct D (generating constructs F and G, respectively). Remarkably, both of these 1 nt deletions completely reversed the upregulation of pre-mRNA. Therefore, we conclude that accumulation of pre-mRNA from PTC+ TCR-β genes is not a consequence of ESE disruption, but rather is caused by premature termination of the open reading frame.

Discussion

In this report, we demonstrate that mRNA reading frame disruption can lead to increases in precursor RNA levels at their sites of transcription. Our study thus unambiguously demonstrates that lack of an intact open reading frame can have *intranuclear* consequences for RNA metabolism. Intriguingly, this effect is independent of PTC position within the transcript, and the introns that remain included can be a long distance upstream of either the PTC or the mutation that induced it. These findings have important implications for the subcellular compartmentalization of gene expression.

One mechanism by which some nonsense mutations lead to alterations in splicing is by chance disruption of ESEs (reviewed in Maquat, 1996; Valentine, 1998; Liu et al., 2001). By destroying the binding site for an individual splicing factor, such mutations directly interfere with the process of exon definition and can thereby cause skipping of the affected exon or retention of an adjacent intron. Although this is clearly a mechanism by which nonsense codons act on some transcripts, we demonstrated by several criteria that the elevation of TCR-β pre-mRNA levels by PTCs is not due to ESE disruption (Figures 7 and 8). We believe it also unlikely that ESE disruption accounts for PTC+ pre-mRNA accumulation at the Ig-μ locus. The mutations that generated those PTCs (two point mutations and a single and a double base-pair deletion) were located in three different exons (see Figure 1A), yet all four PTC+ alleles exhibited similar increases in unspliced μ RNA levels independent of which intron (VL or JC) was examined (Figure 4). That all four mutations would disrupt ESEs acting to such similar extents on two different introns seems extremely unlikely. Furthermore, neither the X54 nor U30 mutation is in an exon that flanks the VL or JC intron. Because the effectiveness of splicing enhancers is highly distance dependent (Tian and Maniatis, 1994; Graveley et al.,

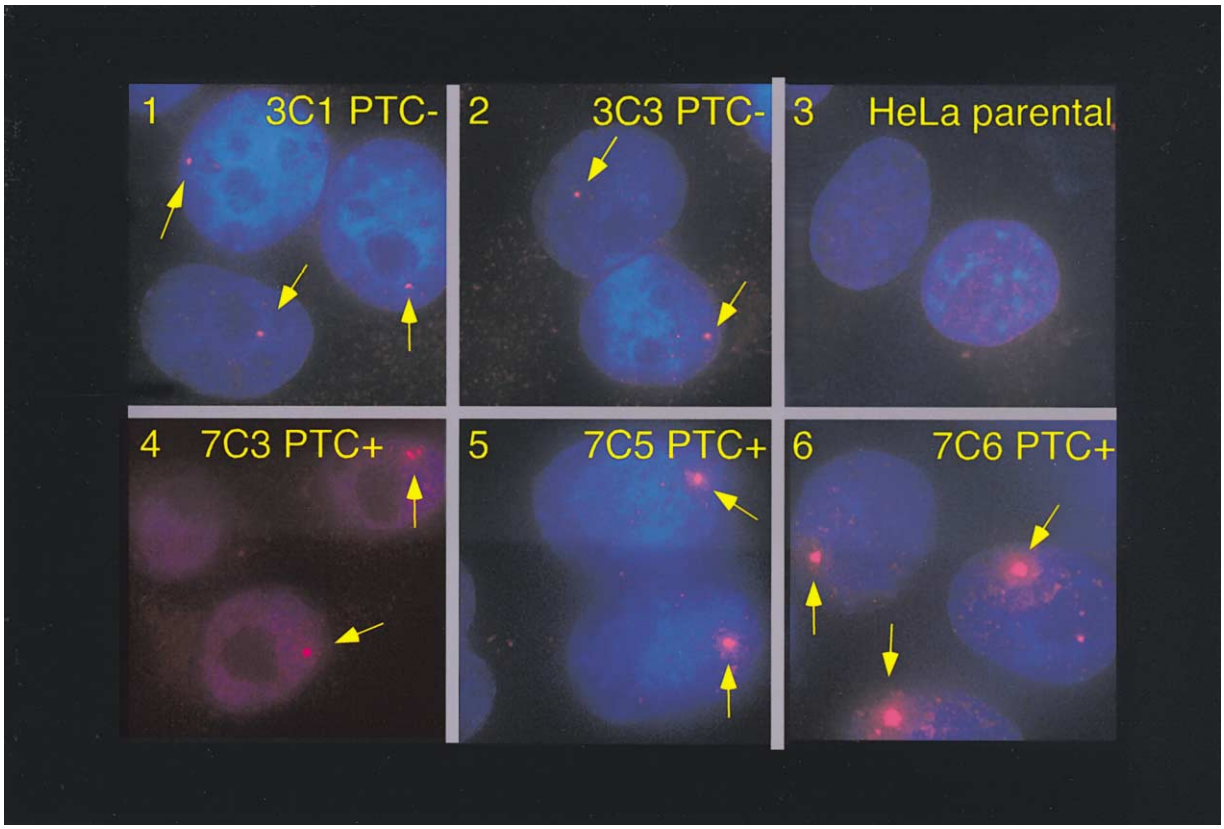

Figure 6. Visualization by FISH of TCR-β RNA in HeLa Cell Lines Stably Transfected with PTC+ and PTC− TCR-β Minigenes

Each cell line was fixed and hybridized to tetramethyl-rhodamine-labeled nick-translated probes (red) specific to the TCR-β portion of the minigene, and DNA stained with Hoechst dye (blue). Images were taken throughout all focal planes containing cellular material ($z > 25$, $\Delta z = 0.2$ μ), deconvolved, and projected onto a single plane (shown here). Fluorescent signals at the transcription sites are marked by arrows. All panels are from a single experiment and have identical fluorescence intensity scaling to allow for direct comparison.

1998), it would be surprising that disruption of an enhancer in the fourth exon would have almost identical effects on the splicing of both the first and second introns. Although there are documented splicing enhancers in the Ig-μ C4 and M2 exons (Watakabe et al., 1993; Mayeda et al., 1999), those enhancers are significantly downstream of all the PTCs examined in our study. Thus, the simplest interpretation of the data is that the accumulation of PTC+ Ig-μ pre-mRNA results from the same enigmatic reading frame-dependent mechanism that acts on TCR-β transcripts.

Is the elevation of pre-mRNA in response to reading frame disruption a general property of transcripts from all genes? To our knowledge, the only other case in which the accumulation of pre-mRNA in response to PTCs has been clearly documented by a quantitative method (RPA) is for transcripts from the minute virus of mice (MVM) (Gersappe et al., 1999; Gersappe and Pintel, 1999). Although RT-PCR is only semiquantitative, and has been specifically shown to artifactually report changes in RNA levels in response to some nonsense codons (Valentine and Heflich, 1997), a PTC-induced

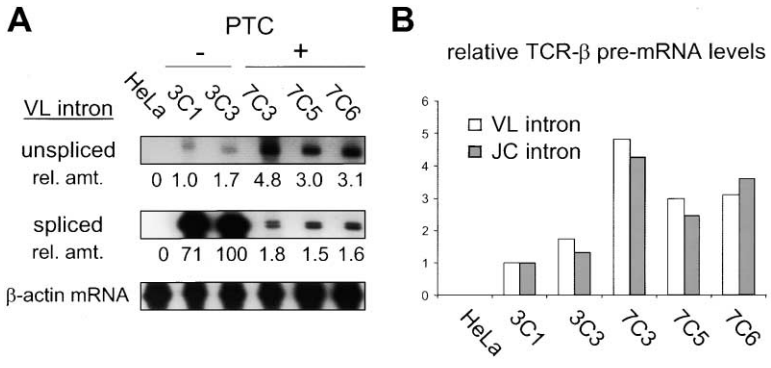

Figure 7. Quantification of Spliced and Unspliced PTC− and PTC+ TCR-β RNA by RNase Protection Analysis

(A) 10 μg total cellular RNA isolated from PTC− (3C1 and 3C3) and PTC+ (7C3, 7C5, and 7C6) HeLa cell lines was hybridized with a VL probe (25 fmoles) and a human β-actin probe (25 fmoles). The indicated levels of pre-mRNA (containing the VL intron) were determined by normalizing against β-actin mRNA and correcting for relative TCR-β transcription rates (see Figure 5B).

(B) Summary of relative TCR-β pre-mRNA levels determined by RNase protection analyses using probes TCR-β VL intron (white) and JC intron (gray) probes (Figure 5A).

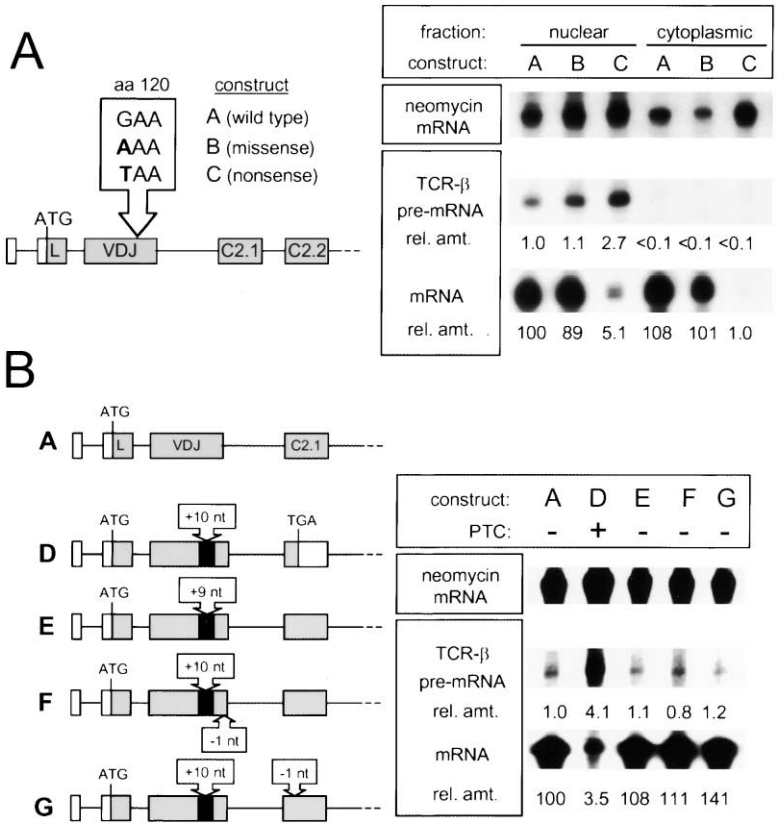

Figure 8. Only Nonsense Codons Induce Higher Levels of Unspliced TCR-β RNA

(A) RPA of nuclear and cytoplasmic RNA (5 μg) isolated from HeLa cell lines obtained by stable transfection with constructs A, B, and C. RNA samples were hybridized with VL and neomycin (internal control) probes (25 fmol, each). Indicated levels of pre-mRNA (containing the VL intron) were determined by normalizing against neomycin mRNA. Average values from three independent assays are shown for each cell line.

(B) RPA of total cellular RNA (5 μg) isolated from HeLa cells transiently transfected with the constructs shown. Probes, hybridization conditions, and result quantification were as in (A).

increase in levels of unspliced Ig-κ transcripts has been documented in B lymphocytes by this method (Lozano et al., 1994; Aoufouchi et al., 1996). It should be noted that the Ig-μ, TCR-β, and Ig-κ genes all commonly acquire PTCs as a consequence of programmed rearrangement during lymphocyte development (Li and Wilkinson, 1998). To date, RT-PCR studies examining transcripts from various nonrearranging genes, including triosephosphate isomerase, β-globin, adenine phosphoribosyltransferase, and androgen-receptor, have not detected increases in pre-mRNA levels in response to PTCs (Maquat, 1995, and references therein). In the future, it will be important to use more quantitative methods to assess whether pre-mRNA upregulation is an effect specific to certain rearranging and viral genes, or whether it is instead a more general response.

Given the prevailing view that translation is limited to the cytoplasm, our finding that premature reading frame termination can influence cotranscriptional events occurring deep in the nuclear interior is paradoxical. We offer two models that may explain this enigma. One model posits that there is a mechanism by which PTC recognition on the cytoplasmic side of the nuclear envelope (by the cytoplasmic translation machinery) feeds back to induce pre-mRNA accumulation at PTC+ gene loci in the nucleus. A rate-limiting event, such as PTC recognition, at the nuclear periphery could thereby back up PTC+ mRNAs to their sites of transcription, thus delaying processing and/or release of newly synthesized RNAs. Alternatively, the signal could be a classical feedback loop that specifically directs alterations in pre-mRNA processing efficiency at PTC+ loci. Regardless of the nature of the signal, such cytoplasmic PTC recognition requires the existence of some physical connection between the nuclear pores and the gene locus; otherwise, it is difficult to envision how the signal could specifically affect PTC+ and not PTC− loci within the same cell, as has been shown for TCR-β transcripts in T lymphocytes (Carter et al., 1995). One possibility is that mRNAs travel from the transcription site to the nuclear periphery along defined tracks (Lawrence et al., 1989; Meier and Blobel, 1992; Murti et al., 1993). However, the existence of such tracks is controversial, and several more recent studies favor instead a purely diffusional intranuclear mRNA transport mechanism (Politz and Pederson, 2000). In our study, we were unable to detect either PTC+ RNA accumulation at the nuclear periphery or RNA localization along any track-like structures (Figures 2 and 6).

An alternate explanation for how mRNA reading frame can affect cotranscriptional events is that eukaryotic cells can detect ORFs (and hence PTCs) within the nucleus proper. This task could be carried out by intranuclear ribosomes, or by an as yet unknown nuclear species with frame-reading capacity (Urlaub et al., 1989). Although numerous studies from the 1960's and 1970's were consistent with the possibility of intranuclear translation (for review, see Goild, 1978), the evidence was ambiguous (for review, see Allen, 1978). More recently, the possibility of nuclear translation has been rekindled by the finding that charged tRNAs and translation initiation factors are found in the nucleus (Etchison and Etchison, 1987; Lund and Dahlberg, 1998; Dostie et al., 2000). If translation does occur inside the nucleus,

where would it occur? One possibility is the nucleolus, as that is where ribosomal subunits are assembled (Pederson and Politz, 2000). However, because most polyA+ RNA is excluded from the nucleolus, it seems unlikely that mRNAs normally traffic through this structure to be scanned for PTCs. A second possibility, more consistent with our data, is that ORF recognition occurs near the site of transcription. In support of this notion, the translation initiation factors eIF4E and eIF4G have both been localized to nuclear speckles (Etchison and Etchison, 1987; Dostie et al., 2000), and some lines of evidence suggest that translation may be coupled with transcription in the nuclei of the slime mold *Dictyostelium discoideum* (Mangiarotti, 1999) and mammalian tissue-culture cells (Iborra et al., 2001).

Why does disruption of mRNA reading frame lead to accumulation of unspliced Ig and TCR RNA near the site of transcription? One demonstrated consequence of splice and polyadenylation site mutations is accumulation of nascent RNAs near their site of synthesis (Custodio et al., 1999; Johnson et al., 2000). Thus, efficient RNA processing is apparently required for rapid release of nascent transcripts from the transcription site. Yet, because no complete ORF is physically established until all the introns have been excised, it is difficult to imagine a mechanism by which ORF recognition could directly affect the earlier process of pre-mRNA splicing. In fact, our finding that PTCs can increase the levels of unspliced RNA harboring introns *upstream* of the PTC argues strongly against direct splicing inhibition in *cis* being the explanation for PTC+ pre-mRNA accumulation. Rather, PTCs may instead act in *trans* to increase precursor mRNA levels. For example, if premature termination of translation causes PTC+ mRNAs to accumulate near the transcription site, this could result in local sequestration of factors required for either pre-mRNA splicing or pre-mRNA degradation. Consistent with this idea, a specific pathway for nuclear pre-mRNA degradation was recently found to exist in yeast, and inhibition of that pathway leads to pre-mRNA accumulation (Bousquet-Antonelli et al., 2000).

Is the accumulation of pre-mRNA in response to PTCs triggered by the NMD RNA surveillance pathway? Although this is an appealing idea, it remains to be tested directly. In support of this idea, we found that all in-frame nonsense codons that triggered the NMD response also caused pre-mRNA induction, whereas missense and out-of-frame nonsense codons failed to trigger either response. However, against this simple notion is the finding the PTC in the N89 Ig-μ cell line only weakly triggered NMD but strongly upregulated pre-mRNA (Figure 4). Furthermore, PTCs appear to inhibit MVM RNA splicing without triggering any detectable NMD response (Gersappe et al., 1999; Gersappe and Pintel, 1999). The ability of reading frame disruptions to induce pre-mRNA accumulation deep inside the nucleus is an intriguing phenomenon that challenges our current view of how gene expression events are compartmentalized. Future studies will be directed toward determining where nonsense codons in TCR and Ig transcripts are recognized within the cell, and whether this recognition event results in a block in RNA splicing, impaired release from transcriptional complexes, increased pre-mRNA stability, or a combination of these events.

Experimental Procedures

Cell Lines and Plasmids

Mouse Ig-μ hybridoma cell lines (Connor et al., 1993; Connor et al., 1994) were kindly provided by Dr. Marc Shulman (University of Toronto). TCR-β minigenes used in Figures 5–7 correspond to constructs A (β-333; PTC−) and C (β-337; PTC+) described by (Li et al., 1997), respectively. For Figure 8, constructs A (β-290) and D (β-291) are pAC/IF and pAc/FS2, respectively, from (Carter et al., 1996). All other constructs were generated by PCR-mediated site-directed mutagenesis of either A or D.

Probes for run-on, Northern and FISH analyses of Ig-μ and TCR-β transcripts were derived from pRSp6 (Ochi et al., 1983a) and plasmids containing mouse Vβ8.1 (Carter et al., 1996), respectively. Probes for Northern blotting and RPA of endogenous human β-actin transcripts were derived from plasmid pAC1 (rat β-actin cDNA; gift from Dr. Susan Birren, Brandeis University) and plasmid G-98 (human β-actin cDNA), respectively. Probes for Ig-κ and mouse β-actin were derived from pRTk1 (Ochi et al., 1983b) and pβ-actin (pGEM2 containing the mouse β-actin cDNA, a gift from Naomi Rosenberg, Tufts Univ. Medical School), respectively. For nuclear run-on assays, antisense ssDNA and riboprobes were generated from fragments of the μ (from pRSp6) and κ (from pRTk1) genes inserted into pGEM 7zf (Promega).

Stable and Transient Transfections

HeLa cells were transiently and stably transfected with TCR-β gene constructs using lipofectamine (Gibco-BRL). For transient transfections, 0.3–1.0 μg plasmid was used to transfect ~80% confluent HeLa cells in 60 mm diameter plates overnight; cells were incubated one day further in new media prior to RNA harvesting. Stable transfections were performed identically, except that cells were ~10% confluent in 6-well plates and were incubated with 0.5 mg/ml G418 from the day after transfection until fully viable (selected) cell lines were obtained.

Nuclear Run-On Analysis

Isolation of nuclei was as described by Panning and Smiley (1993). Per run-on sample, 0.5–1.0 $\times$ 10^7 nuclei were labeled with α^{32}P-UTP as described by Smibert and Smiley (1990). Subsequently, total RNA was isolated and 0.1–2.0 $\times$ 10^7 cpm used for hybridization of a nylon filter on which 5–10 μg of linearized, denatured plasmid DNA (Figures 1B and 5B), 2–4 μg of single stranded DNA probe, or 1 μg of riboprobe (Figure 1C) had been immobilized per slot. Hybridization conditions were typically 40 hr at 55°C in 50% formamide, 5xSSC, 0.1% SDS, 1 mM EDTA, 10 mM Tris (pH 7.5), 100 μg/ml *E. coli* tRNA, and 100 μg/ml salmon sperm DNA. Subsequently, filter strips were washed extensively in 2xSSC at 68°C and incubated with 50 μg/ml RNase A for 30 min at 37°C. Signals were visualized and quantified by PhosphorImager scanning (Molecular Dynamics).

Northern Analysis

Total cellular RNA (5 μg) was separated in a 1% agarose/formaldehyde gel, transferred to a nylon membrane, and probed with ^{32}P-labeled, random-primed DNA fragments. Ig-μ and mouse β-actin mRNAs were probed with the 4.6 kb XbaI fragment of pBCL-1 (Landolfi et al., 1986) and the 2 kb PstI fragment of pβ-actin, respectively. A PCR product encompassing only the VDJ region of pβ332 and a PCR product containing exons 2 and 3 of rat β-actin allowed for specific detection of TCR-β minigene mRNA and endogenous human β-actin mRNA, respectively. Blots were visualized and quantified by PhosphorImager scanning.

FISH

B cell hybridomas were grown in suspension in DMEM medium (Gibco BRL) supplemented with 12% bovine newborn calf serum (Gibco BRL), 100 U/mL penicillin, 100 U/mL streptomycin, and 10 μMβ-mercaptoethanol, harvested by centrifugation, and allowed to settle on poly-L-lysine-coated coverslips. HeLa cells were directly grown on coverslips in DMEM medium supplemented with 10% fetal bovine serum, 0.3 mg/ml L-glutamine, 100 U/mL penicillin, and 100 U/mL streptomycin. Media for transfected HeLa cells also contained 400 μg/mL Geneticin (G418 sulfate). For both cell types, conditions

for fixation, permeabilization, hybridization, and posthybridization washes were as described (Custodio et al., 1999). The probe used in Figure 6 was pβ322 nick-translated in the presence of rhodamine-coupled dUTP (Molecular Probes) under conditions yielding an average fragment length of 200 to 300 nt. The genomic (Figure 2A) and intronic (Figure 2C) probes for Ig-μ were generated similarly from pRSp6 and the 3.4 kb *Xba*I fragment of pRSp6, respectively. Typically 4 to 8 ng/μl probe was used per coverslip. Hybridoma cells were subsequently immunolabeled with FITC-conjugated goat anti-mouse IgM antibody (Jackson Laboratories); DNA was stained in all cells with Hoechst dye (bis-benzimide; Sigma). Images were acquired in multiple focal planes ($\Delta z = 0.2–0.4$ μm, 40–60 planes), deconvolved, and subsequently projected in two dimensions (as shown in Figures 2A, 2C, and 6), using a DeltaVision microscopy system and accompanying software. Quantification of Ig-μ fluorescence signals (Figures 2B and 2D) is described in Results. For the detailed quantification of N114 and Sp6 spots (Figure 3), four fields of cells from a single FISH experiment using the intronic probe were analyzed by drawing three dimensional polygons around each visible transcription spot using the DeltaVision™ software. The total intensity of each transcription spot was then determined by summing all pixel intensities within the polygon volume.

RNase Protection Assays

Riboprobes schematized in Figures 1A and 5A spanned 62–140 nt of the indicated intron, plus 60–90 nt of the adjacent exon. A probe complementary to the last 70 nt of exon 4 and first 70 nt of exon 5 in mouse β-actin mRNA was generated using PCR primers generously provided by Nicolas Charlet-Berguerand (CNRS, France). The riboprobe for detecting human β-actin mRNA was complementary to nt 135–169 in exon 3 (Accession # X00351). Neomycin transcripts, which contained SV-40 3′ UTR sequences, were detected with a probe complementary to the last 46 nt of the SV-40 small t intron, plus 200 nt of the downstream SV40 exon. All riboprobes were transcribed using a 1:5 or 1:7 ratio of α-^{32}P-labeled to unlabeled UTP, gel-purified and used for RPA as previously described (Dumas et al., 1996; Lindsey and Wilkinson, 1996). Gels were visualized and quantified with either a Molecular Dynamics PhosphorImager or a Packard Instant Imager. Titration experiments revealed that 12 fmol of each Ig-μ probe, 10 fmol of β-actin probe, 25 fmol of TCR-β probe, and 25 fmol of Neomycin probe (the amounts used in all experiments) yielded linear responses with up to 9–10 μg of total cellular RNA (data not shown).

Acknowledgments

As noted in the text, we are indebted to many individuals for providing necessary reagents. We particularly thank Dr. Marc Shulman for providing the B cell hybridomas and many helpful discussions. This work was supported by a Swiss National Foundation Postdoctoral Fellowship (O.M.), NIH training grant #5 T32 GM07122(C.M.-C.), National Science Foundation Grant MCB-9808936 (M.F.W.), NIH grant GM-58595 (M.F.W.), and a David and Lucille Packard Fellowship (M.J.M.). M.J.M. is an assistant investigator with the Howard Hughes Medical Institute.

Received December 22, 2000; revised May 17, 2001.

References

Allen, W. (1978). Does protein synthesis occur within the nucleus? Unambiguous evidence is still needed. Trends Biol. Sci. *3*, N225–N228.

Aoufouchi, S., Yelamos, J., and Milstein, C. (1996). Nonsense mutations inhibit RNA splicing in a cell-free system: recognition of mutant codon is independent of protein synthesis. Cell *85*, 415–422.

Baserga, S.J., and Benz, E.J., Jr. (1992). Beta-globin nonsense mutation: deficient accumulation of mRNA occurs despite normal cytoplasmic stability. Proc. Natl. Acad. Sci. USA *89*, 2935–2939.

Belgrader, P., Cheng, J., Zhou, X., Stephenson, L.S., and Maquat, L.E. (1994). Mammalian nonsense codons can be cis effectors of nuclear mRNA half- life. Mol. Cell. Biol. *14*, 8219–8228.

Belgrader, P., and Maquat, L.E. (1994). Nonsense but not missense mutations can decrease the abundance of nuclear mRNA for the mouse major urinary protein, while both types of mutations can facilitate exon skipping. Mol. Cell. Biol. *14*, 6326–6336.

Bousquet-Antonelli, C., Presutti, C., and Tollervey, D. (2000). Identification of a regulated pathway for nuclear pre-mRNA turnover. Cell *102*, 765–775.

Brogna, S. (1999). Nonsense mutations in the alcohol dehydrogenase gene of Drosophila melanogaster correlate with an abnormal 3′ end processing of the corresponding pre-mRNA. RNA *5*, 562–573.

Buzina, A., and Shulman, M.J. (1999). Infrequent translation of a nonsense codon is sufficient to decrease mRNA level. Mol. Biol. Cell *10*, 515–524.

Carter, M.S., Doskow, J., Morris, P., Li, S., Nhim, R.P., Sandstedt, S., and Wilkinson, M.F. (1995). A regulatory mechanism that detects premature nonsense codons in T-cell receptor transcripts in vivo is reversed by protein synthesis inhibitors in vitro. J. Biol. Chem. *270*, 28995–29003.

Carter, M.S., Li, S., and Wilkinson, M.F. (1996). A splicing-dependent regulatory mechanism that detects translation signals. EMBO J. *15*, 5965–5975.

Cheng, J., and Maquat, L.E. (1993). Nonsense codons can reduce the abundance of nuclear mRNA without affecting the abundance of pre-mRNA or the half-life of cytoplasmic mRNA. Mol. Cell. Biol. *13*, 1892–1902.

Connor, A., Collins, C., Jiang, L., McMaster, M., and Shulman, M.J. (1993). Isolation of new nonsense and frameshift mutants in the immunoglobulin mu heavy-chain gene of hybridoma cells. Somat. Cell Mol. Genet. *19*, 313–320.

Connor, A., Wiersma, E., and Shulman, M.J. (1994). On the linkage between RNA processing and RNA translatability. J. Biol. Chem. *269*, 25178–25184.

Cooper, T.A., and Mattox, W. (1997). The regulation of splice-site selection, and its role in human disease. Am. J. Hum. Genet. *61*, 259–266.

Custodio, N., Carmo-Fonseca, M., Geraghty, F., Pereira, H.S., Grosveld, F., and Antoniou, M. (1999). Inefficient processing impairs release of RNA from the site of transcription. EMBO J. *18*, 2855–2866.

Dietz, H.C., and Kendzior, R.J., Jr. (1994). Maintenance of an open reading frame as an additional level of scrutiny during splice site selection. Nat. Genet. *8*, 183–188.

Dietz, H.C., Valle, D., Francomano, C.A., Kendzior, R.J., Jr., Pyeritz, R.E., and Cutting, G.R. (1993). The skipping of constitutive exons in vivo induced by nonsense mutations. Science *259*, 680–683.

Dirks, R.W., Daniel, K.C., and Raap, A.K. (1995). RNAs radiate from gene to cytoplasm as revealed by fluorescence in situ hybridization. J. Cell Sci. *108*, 2565–2572.

Dostie, J., Lejbkowicz, F., and Sonenberg, N. (2000). Nuclear eukaryotic initiation factor 4E (eIF4E) colocalizes with splicing factors in speckles. J. Cell Biol. *148*, 239–247.

Dumas, S., Le Hir, H., Bodeau-Pean, S., Hirsch, E., Thermes, C., and Mallet, J. (1996). New species of human tyrosine hydroxylase mRNA are produced in variable amounts in adrenal medulla and are overexpressed in progressive supranuclear palsy. J. Neurochem. *67*, 19–25.

Etchison, D., and Etchison, J.R. (1987). Monoclonal antibody-aided characterization of cellular p220 in uninfected and poliovirus-infected HeLa cells: subcellular distribution and identification of conformers. J. Virol. *61*, 2702–2710.

Frischmeyer, P.A., and Dietz, H.C. (1999). Nonsense-mediated mRNA decay in health and disease. Hum. Mol. Genet. *8*, 1893–1900.

Gersappe, A., Burger, L., and Pintel, D.J. (1999). A premature termination codon in either exon of minute virus of mice P4 promoter-generated pre-mRNA can inhibit nuclear splicing of the intervening intron in an open reading frame-dependent manner. J. Biol. Chem. *274*, 22452–22458.

Gersappe, A., and Pintel, D.J. (1999). A premature termination codon interferes with the nuclear function of an exon splicing enhancer

in an open reading frame-dependent manner. Mol. Cell. Biol. *19*, 1640–1650.

Goild, J. (1978). Does protein synthesis occur within the nucleus? Good evidence that it does. Trends Biol. Sci. *3*, N225–N228.

Graveley, B.R., Hertel, K.J., and Maniatis, T. (1998). A systematic analysis of the factors that determine the strength of pre-mRNA splicing enhancers. EMBO J. *17*, 6747–6756.

Hentze, M.W., and Kulozik, A.E. (1999). A perfect message: RNA surveillance and nonsense-mediated decay. Cell *96*, 307–310.

Iborra, F.J., Jackson, D.A., and Cook, P.R. (2001). Coupled Transcription and Translation Within Nuclei of Mammalian Cells. Science, in press.

Johnson, C., Primorac, D., McKinstry, M., McNeil, J., Rowe, D., and Lawrence, J.B. (2000). Tracking COL1A1 RNA in osteogenesis imperfecta. splice-defective transcripts initiate transport from the gene but are retained within the SC35 domain. J. Cell Biol. *150*, 417–432.

Jolly, C., Robert-Nicoud, M., and Vourc'h, C. (1998). Contribution of growing RNA molecules to the nuclear transcripts foci observed by FISH. Exp. Cell Res. *238,* 299–304.

Kessler, O., and Chasin, L.A. (1996). Effects of nonsense mutations on nuclear and cytoplasmic adenine phosphoribosyltransferase RNA. Mol. Cell. Biol. *16*, 4426–4435.

Landolfi, N.F., Capra, J.D., and Tucker, P.W. (1986). Interaction of cell-type-specific nuclear proteins with immunoglobulin VH promoter region sequences. Nature *323*, 548–551.

Lawrence, J.B., Singer, R.H., and Marselle, L.M. (1989). Highly localized tracks of specific transcripts within interphase nuclei visualized by in situ hybridization. Cell *57*, 493–502.

Le Hir, H., Izaurralde, E., Maquat, L.E., and Moore, M.J. (2000). The spliceosome deposits multiple proteins 20–24 nucleotides upstream of mRNA exon-exon junctions. EMBO J. *19*, 6860–6869.

Li, S., Leonard, D., and Wilkinson, M.F. (1997). T cell receptor (TCR) mini-gene mRNA expression regulated by nonsense codons: a nuclear-associated translation-like mechanism. J. Exp. Med. *185*, 985–992.

Li, S., and Wilkinson, M.F. (1998). Nonsense surveillance in lymphocytes? Immunity *8*, 135–141.

Lim, S.K., Sigmund, C.D., Gross, K.W., and Maquat, L.E. (1992). Nonsense codons in human beta-globin mRNA result in the production of mRNA degradation products. Mol. Cell. Biol. *12*, 1149–1161.

Lindsey, J.S., and Wilkinson, M.F. (1996). Pem: a testosterone- and LH-regulated homeobox gene expressed in mouse Sertoli cells and epididymis. Dev. Biol. *179*, 471–484.

Liu, H.X., Cartegni, L., Zhang, M.Q., and Krainer, A.R. (2001). A mechanism of exon skipping caused by nonsense or missense mutations in *BRCA1* and other genes. Nat. Genet. *27*, 55–58.

Lozano, F., Maertzdorf, B., Pannell, R., and Milstein, C. (1994). Low cytoplasmic mRNA levels of immunoglobulin kappa light chain genes containing nonsense codons correlate with inefficient splicing. EMBO J. *13*, 4617–4622.

Lund, E., and Dahlberg, J.E. (1998). Proofreading and aminoacylation of tRNAs before export from the nucleus. Science *282*, 2082–2085.

Mangiarotti, G. (1999). Coupling of transcription and translation in Dictyostelium discoideum nuclei. Biochemistry *38*, 3996–4000.

Maquat, L.E. (1995). When cells stop making sense: effects of nonsense codons on RNA metabolism in vertebrate cells. RNA *1*, 453–465.

Maquat, L.E. (1996). Defects in RNA splicing and the consequence of shortened translational reading frames. Am. J. Hum. Genet. *59*, 279–286.

Mayeda, A., Screaton, G.R., Chandler, S.D., Fu, X.D., and Krainer, A.R. (1999). Substrate specificities of SR proteins in constitutive splicing are determined by their RNA recognition motifs and composite pre-mRNA exonic elements. Mol. Cell. Biol. *19*, 1853–1863.

Meier, U.T., and Blobel, G. (1992). Nopp140 shuttles on tracks between nucleolus and cytoplasm. Cell *70*, 127–138.

Moriarty, P.M., Reddy, C.C., and Maquat, L.E. (1998). Selenium deficiency reduces the abundance of mRNA for Se-dependent glutathione peroxidase 1 by a UGA-dependent mechanism likely to be nonsense codon-mediated decay of cytoplasmic mRNA. Mol. Cell. Biol. *18*, 2932–2939.

Murti, K.G., Brown, P.S., Ratner, L., and Garcia, J.V. (1993). Highly localized tracks of human immunodeficiency virus type 1 Nef in the nucleus of cells of a human CD4+ T-cell line. Proc. Natl. Acad. Sci. USA *90*, 11895–11899.

Nagy, E., and Maquat, L.E. (1998). A rule for termination-codon position within intron-containing genes: when nonsense affects RNA abundance. Trends Biochem. Sci. *23*, 198–199.

Ochi, A., Hawley, R.G., Hawley, T., Shulman, M.J., Traunecker, A., Kohler, G., and Hozumi, N. (1983a). Functional immunoglobulin M production after transfection of cloned immunoglobulin heavy and light chain genes into lymphoid cells. Proc. Natl. Acad. Sci. USA *80*, 6351–6355.

Ochi, A., Hawley, R.G., Shulman, M.J., and Hozumi, N. (1983b). Transfer of a cloned immunoglobulin light-chain gene to mutant hybridoma cells restores specific antibody production. Nature *302*, 340–342.

Panning, B., and Smiley, J.R. (1993). Activation of RNA polymerase III transcription of human Alu repetitive elements by adenovirus type 5: requirement for the E1b 58-kilodalton protein and the products of E4 open reading frames 3 and 6. Mol. Cell. Biol. *13*, 3231–3244.

Pederson, T., and Politz, J.C. (2000). The nucleolus and the four ribonucleoproteins of translation. J. Cell Biol. *148*, 1091–1095.

Politz, J.C., and Pederson, T. (2000). Review: movement of mRNA from transcription site to nuclear pores. J. Struct. Biol. *129*, 252–257.

Shiga, N., Takeshima, Y., Sakamoto, H., Inoue, K., Yokota, Y., Yokoyama, M., and Matsuo, M. (1997). Disruption of the splicing enhancer sequence within exon 27 of the dystrophin gene by a nonsense mutation induces partial skipping of the exon and is responsible for Becker muscular dystrophy. J. Clin. Invest. *100*, 2204–2210.

Simpson, S.B., and Stoltzfus, C.M. (1994). Frameshift mutations in the v-src gene of avian sarcoma virus act in cis to specifically reduce v-src mRNA levels. Mol. Cell. Biol. *14*, 1835–1844.

Smibert, C.A., and Smiley, J.R. (1990). Differential regulation of endogenous and transduced beta-globin genes during infection of erythroid cells with a herpes simplex virus type 1 recombinant. J. Virol. *64*, 3882–3894.

Thermann, R., Neu-Yilik, G., Deters, A., Frede, U., Wehr, K., Hagemeier, C., Hentze, M.W., and Kulozik, A.E. (1998). Binary specification of nonsense codons by splicing and cytoplasmic translation. EMBO J. *17*, 3484–3494.

Tian, M., and Maniatis, T. (1994). A splicing enhancer exhibits both constitutive and regulated activities. Genes Dev. *8*, 1703–1712.

Urlaub, G., Mitchell, P.J., Ciudad, C.J., and Chasin, L.A. (1989). Nonsense mutations in the dihydrofolate reductase gene affect RNA processing. Mol. Cell. Biol. *9*, 2868–2880.

Valentine, C.R. (1998). The association of nonsense codons with exon skipping. Mutat. Res. *411*, 87–117.

Valentine, C.R., and Heflich, R.H. (1997). The association of nonsense mutation with exon-skipping in hprt mRNA of Chinese hamster ovary cells results from an artifact of RT-PCR. RNA *3*, 660–676.

Watakabe, A., Tanaka, K., and Shimura, Y. (1993). The role of exon sequences in splice site selection. Genes Dev. *7*, 407–418.

Whitfield, T.T., Sharpe, C.R., and Wylie, C.C. (1994). Nonsense-mediated mRNA decay in Xenopus oocytes and embryos. Dev. Biol. *165*, 731–734.

Zhang, J., Sun, X., Qian, Y., LaDuca, J.P., and Maquat, L.E. (1998a). At least one intron is required for the nonsense-mediated decay of triosephosphate isomerase mRNA: a possible link between nuclear splicing and cytoplasmic translation. Mol. Cell. Biol. *18*, 5272–5283.

Zhang, J., Sun, X., Qian, Y., and Maquat, L.E. (1998b). Intron function in the nonsense-mediated decay of beta-globin mRNA: indications that pre-mRNA splicing in the nucleus can influence mRNA translation in the cytoplasm. RNA *4*, 801–815.